Master-Slave Electric Cart Control System for Maintaining/Improving Physical Strength

Jin-Hua She, *Member, IEEE,* Yasuhiro Ohyama, *Member, IEEE,* and Hiroyuki Kobayashi

IEEE Transactions on Robotics, Vol. 22, No. 3, 2006.

***Abstract*— This paper explains the development of a new-concept three-wheeled electric cart that not only is a means of transportation, but also provides the driver with a way of getting some physical exercise.**

Based on an investigation of the physiological decline accompanying aging, pedaling was chosen to implement the function of maintaining or improving physical strength; and an ergonomically designed pedal unit was mounted on a cart. An interface board that handles inputs and outputs was assembled to simplify the design of the system. Finally, an impedance model was devised to describe the feeling of pushing the pedals, and a bilateral master-slave H_∞ control system was built to control the speed of the cart. Experimental results on a prototype cart demonstrate the effectiveness of pedaling and the usability of the system architecture.

***Index Terms*— Electric cart, aging, motor functions, pedaling, bilateral master-slave system, cooperative man-machine system, H_∞ control.**

I. Introduction

The number of elderly people in Japan is increasing at an unprecedented rate. According to an annual report on aging from the Cabinet Office of the Government of Japan [1], the percentage of old people (over 65 years old) in the population exceeded 7% (aging society) in 1970 and 14% (aged society) in 1994, and reached 19% in 2003. As the average life span of Japanese continues to increase, there is a concomitant marked increase in the number of people who are in fragile health due to age, suffer senile dementia, or are bedridden. Since the medical treatment and care of old people confined to bed is a particularly onerous burden on financial and manpower resources, it is becoming a very serious social problem. Accordingly, the health and welfare of the elderly has become one of the main concerns of the government, and policies dealing with an aging society and their implementation have received considerable attention. In particular, the last decade has seen a rapid rise in public concern about how to establish an environment for the elderly that will facilitate their maintaining and improving their health to ensure a useful and productive old age (i.e., to ensure mental and physical soundness); and a great deal of research and development related to the health and welfare of the elderly is now being carried out.

One part of this research focuses on electric carts, a great variety of which have been developed to improve the ability of old people to get around [2], [3]. However, designers have tended to take a rather short-sighted view by emphasizing convenience and ease of use (the driver just has to push a forward or backward button and steer) while neglecting long-term health effects. That is: almost all commercially available carts were designed solely as a means of transportation, and no consideration was given to an elderly person's need for physical exercise. Unfortunately, a reliance on these carts for getting around can ultimately result in the deterioration of the user's leg and back muscles, thus contributing to, rather than helping to solve, the problem. Hence, it would be difficult to say that currently available carts truly enhance the lifestyle of the elderly by helping them to be more mobile and independent because, in the long run, they simply hasten the descent into a dependent state.

In this study, a new-concept three-wheeled electric cart was developed. It not only is a means of transportation, but also provides the driver with a way of getting some physical exercise. For this purpose, two foot pedals are mounted on the cart, and the load added to the pedals can be adjusted with a speed-adjustment program to suit the physical condition of the driver. So, not only does it help the elderly get around, at the same time it also helps them maintain or improve their physical condition in a natural and enjoyable way. This actively prevents the degeneration of motor functions. As a result, it has salutary effects on both the physiology and psychology of the elderly, which is a benefit to the whole society. This type of cart can thus make a very positive contribution to the aged society.

The paper is organized as follows: Section 2 reviews measures for preventing muscular degeneration due to aging based on an investigation of the physiological deterioration that typically accompanies aging. Section 3 describes a prototype of a new-concept electric cart that was designed based on those results and ergonomics studies. Section 4 concerns the configuration of a bilateral master-slave control system for controlling the speed of the cart. The design of the controller is based on H_∞ control theory. The experimental results on a fabricated cart in Section 5 demonstrate the validity and effectiveness of the design method. Some concluding remarks are made in Section 6.

II. Muscular Degeneration due to Aging and Its Prevention

This section concerns an analysis of muscular degeneration due to aging, and measures to prevent it.

J.-H. She, Y. Ohyama and H. Kobayashi are with the School of Bionics, Tokyo University of Technology, 1404-1 Katakura, Hachioji, Tokyo, 192-0982 Japan (e-mail: {she, ohyama, yagshi}@bs.teu.ac.jp).

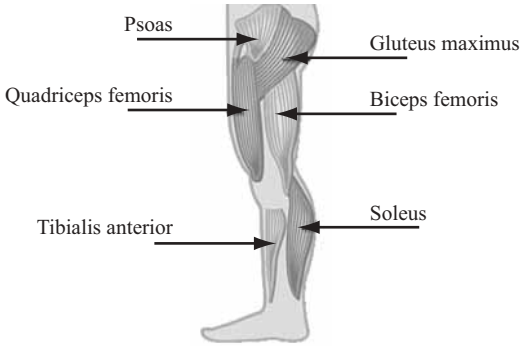

Fig. 1. Walking muscles.

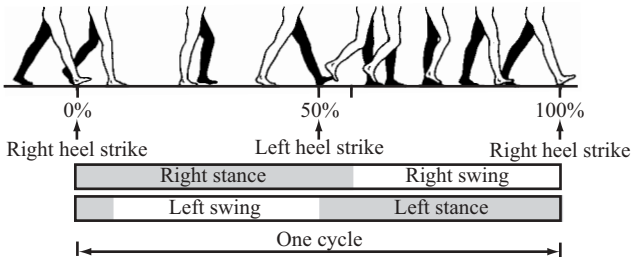

Fig. 2. One cycle of leg movement during walking.

A. Muscular Degeneration due to Aging

The human body changes with age. An analysis of the relationship between muscle volume and aging revealed the following: The muscle volume of the brachial-flexor group is $200 \sim 300$ cm^3 for men and $150 \sim 200$ cm^3 for women of all ages, and seems to be little affected by aging. In contrast, the muscle volume of the femoral-extensor group reaches a maximum during a person's twenties or thirties, and is about 1700 cm^3 for men and 1200 cm^3 for women. Subsequently, the volume gradually decreases, and drops to about 60% of the peak value for people in their seventies [4], [5]. Clearly, the decrease in muscle volume is more marked for lower than for upper limbs. The major cause seems to be that the activity of the arms does not decrease very much with age, whereas people tend to become more sedentary in later life, which causes the leg muscles to atrophy.

Walking is a basic action of daily life involving the use of what are called the walking muscles: loin muscle (psoas), gluteal muscle (gluteus maximus), front thigh muscle (quadriceps femoris), hamstring muscle (biceps femoris), calf muscle (soleus), shin muscle (tibialis anterior) and some others (Fig. 1). When a person walks, each leg moves through a cycle (Fig. 2) of alternating stance and swing phases [6]. In the stance phase, the foot is in contact with the floor; the main muscles employed are the gluteal, front thigh, and calf muscles. In the swing phase, the foot is off the floor and moving forward; the main muscles employed are the gluteal, hamstring, front thigh, and shin muscles.

The loin, front thigh, calf, and shin muscles are the ones that tend to weaken the most with aging. The leg cannot be lifted if the loin, gluteal, and front thigh muscles are too weak; the heel cannot be raised if the calf muscle is too weak; and the toes cannot be raised if the shin muscle is too weak. Muscular degeneration starts in a person's forties and accelerates with aging. For example, according to a study done in metropolitan areas of Japan, the front thigh muscles of people in their seventies are about 28% smaller, and their calf muscles are about 23% smaller, than those of people in their twenties [4].

Muscle tissue contains two types of fibers: slow-twitch and fast-twitch. Slow-twitch fibers provide stamina; while fast-twitch fibers contract rapidly, providing quick power. Fast-twitch fibers tend to atrophy more quickly during the aging process.

B. Prevention Measures

To prevent the degradation of motor functions, the walking muscles that degenerate most rapidly (loin, front thigh, calf, and shin muscles) need to be exercised. Moreover, some thought needs to be given to the special needs of the elderly [5], [7]. Aerobic endurance exercises, such as walking, jogging, etc., train only slow-twitch fibers, and are not much help in preventing the degeneration of fast-twitch fibers due to aging. So, in addition to aerobic exercise, anaerobic exercise, which induces an excitatory state, is needed to arrest the atrophy of fast-twitch fibers. This is why it is strongly recommended that physical exercise for old people include not only jogging or walking for a relatively long time to work the slow-twitch fibers, but also some very short (dozens of seconds) strengthening exercises to work the fast-twitch fibers.

From among the variety of activities available, our attention was drawn to pedaling. When the pedal moves through the downward half of the cycle, the front thigh, hamstring, and calf muscles are worked; when it moves back up, the loin, front thigh, and shin muscles are worked. So, pedaling would seem to be almost the ideal exercise to work the muscles that are liable to degenerate due to aging [8].

Based on these considerations, we decided to mount two foot pedals on an electric cart to provide the driver with a way of exercising the walking muscles.

III. Design of Cart System

This section describes the pedal design, how the pedal load is generated, and the structure of the system.

A commercially available ready-made three-wheeled electric cart, the Everyday Type-S (Araco Corp., Japan; Cart motor: 24 V, 330 W, DENSO Corp., Japan), was selected as the foundation of the system.

A. Pedal Load and Pedal Installation

The two pedals are a commercially available model (JP-350, 95 mm $\times$ 70 mm $\times$ 30 mm). Since we want to focus on exercising the walking muscles, it is natural to consider adding a load to the pedals, which is the amount of additional resistance that the driver feels when the pedals are pushed. There are two types of loads that can be produced: constant and time-varying. A time-varying load, especially one that is responsive to the road conditions, provides the driver with a more enjoyable and more realistic driving experience, thereby making exercise more bearable. That makes a time-varying

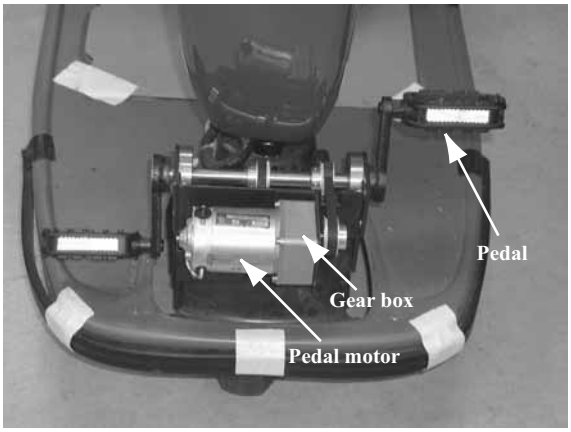

Fig. 3. Pedal unit (pedals and pedal motor).

load more suitable. Furthermore, even though a mechanical connection between the pedals and the drive wheels (as on a bicycle) was deemed to be the most appropriate for the system structure, an electrical connection was employed because it provided greater potential for further development. An electrical connection has the following advantages over a mechanical one:

- Greater flexibility: Since the load is easy to adjust with a program, it can readily be adapted to the state of health of the driver and meet various needs.
- Greater design freedom: In addition to producing a load for the driver, this type of connection can also provide an assist if the need arises. This gives the designer much more freedom.
- Better reliability: Since it does not have the problems of lubrication, abrasion, and mechanical breakdown, the reliability of the whole system is substantially higher.

The pedals are connected to a geared DC motor (24 V, 25 W, Tsukasa Electric Co. Ltd., Japan), which generates the load; and the pedals and motor constitute the pedal unit (Fig. 3).

Some physiological data on the elderly in Japan are shown in Table I [9]. Except for "Height", the items are for a seated person (Fig. 4): "Hip-knee distance" is the distance from the front of the kneecap to the rear of the hip; "Height of seat" is the distance from the bottom of the foot to the hamstring; and "Height of knee" is the distance from the bottom of the foot to the top of the kneecap. The seat reference point is the vertical projection of the rear of the hip onto the seat. The table shows that the proper height of the seat is about $35 \sim 40$ cm. From the optimal pedaling region given by [10] (Fig. 5) and the data in the table, we find that the region for easy pedaling is about $60 \sim 90$ cm forward and $10 \sim 40$ cm below the seat reference point. The pedal unit was attached to the cart using these figures as a starting point, and then the position was adjusted based on the results of test rides. In the final configuration, the seat was mounted 40 cm above the base of the cart; and the pedal unit was mounted 13 cm above the base and 80 cm in front of the seat reference point. So, the vertical distance from the center of the pedal unit to the seat is 27 cm. Table I and Fig. 5 show that this provides optimal pedaling for a Japanese elderly of average height.

TABLE I
STATISTICS ON THE ELDERLY IN JAPAN.

Year	2000	2001
Height [cm]	154.3	155.0
Hip-knee distance [cm]	45.6	44.1
Height of seat [cm]	37.8	37.6
Height of knee [cm]	45.0	45.3

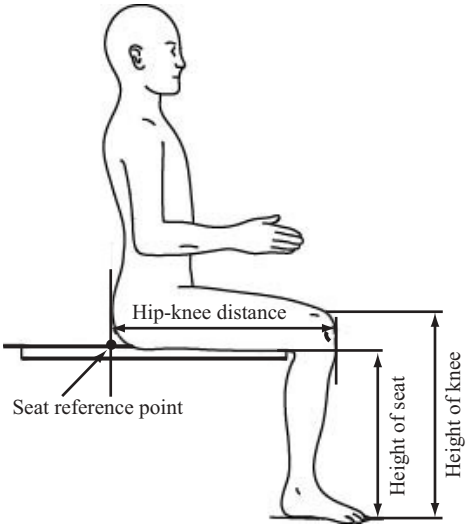

Fig. 4. Definitions [9].

B. Interface Design

Two optical encoders measure the rotational angles of the pedal and cart motors (8000 and 2400 pulses per revolution, respectively). To keep the system configuration simple while allowing easy implementation of various functions, we built an interface board to handle all the inputs and outputs of the pedal and cart motors (Fig. 6). To allow room for system expansion and to enable the intelligent processing of information, the board has a PIC microcontroller (PIC16C74, [11]), which contains an 8-bit 20-MHz CPU, $4\ \mathrm{K} \times 14$ bits of program memory, 192 bytes of data memory, 2 PWM modules, a synchronous serial port (SSP), a universal synchronous-asynchronous receiver transmitter (USART), serial communication ports, a parallel slave port (PSP), a communication port, 8 input channels for an 8-bit A/D module, and 5 I/O ports. In this study, the PIC

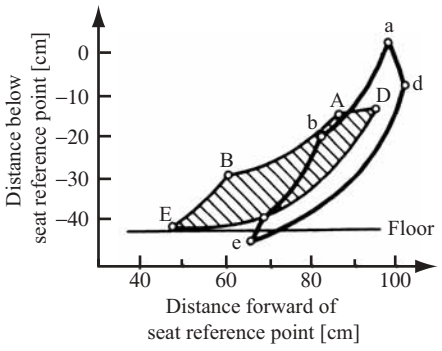

Fig. 5. Optimal pedaling region (Capital: heel position; Small: toe position).

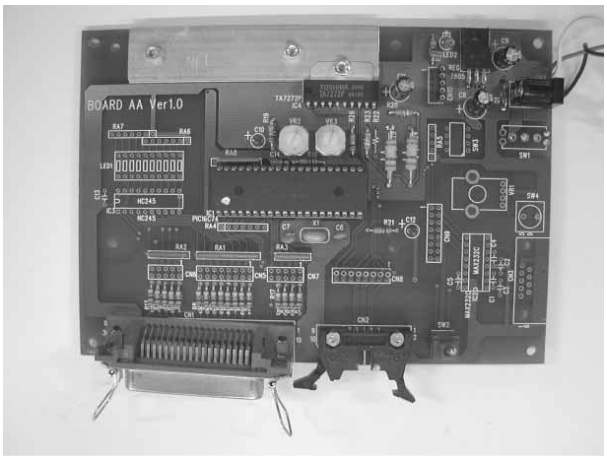

(a) Photo

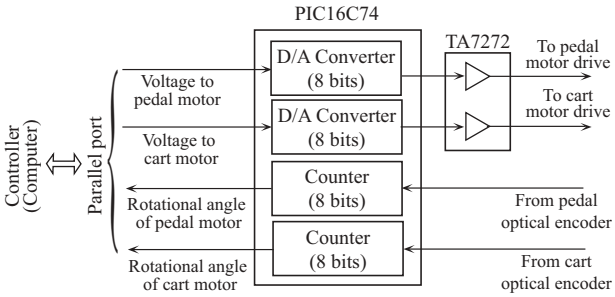

(b) Block diagram

Fig. 6. Interface board.

was programmed to implement the following functions:

- Two serial communication ports are used as two counters to collect information on rotational angle from the optical encoders of the pedal and cart motors; and the information is then sent to the computer (controller) over parallel connections.
- The computer sends the control inputs for the pedal and cart motors to the PIC over two parallel connections; and the PIC converts them to analog voltages. The 2 PWM modules function as 8-bit D/A converters.

These functions are implemented using PIC assembler language. Finally, an operational amplifier, TA7272 [12], adjusts the level of the control signals ($-5 \sim +5$ V) to that required by the motor drives ($-24 \sim +24$ V); and sends them to the motor drives.

Since many of the resources of the PIC remain available for the developer to use, a great variety of functions can be implemented directly on the interface board. For example, the control system could monitor the driver's physical condition in real time and adjust operation accordingly. So, the board provides the developer with great freedom in system development and an environment for system integration.

An electric cart modified as described above is shown in Fig. 7.

IV. Configuration and Design of Control System

This section explains the configuration of the cart control system. After a model of the system is presented, an impedance model is devised to describe the feeling of pushing the pedals, and the control problem is formulated using the H_∞ control theory framework. An H_∞ controller is obtained using the linear matrix inequality (LMI) algorithm.

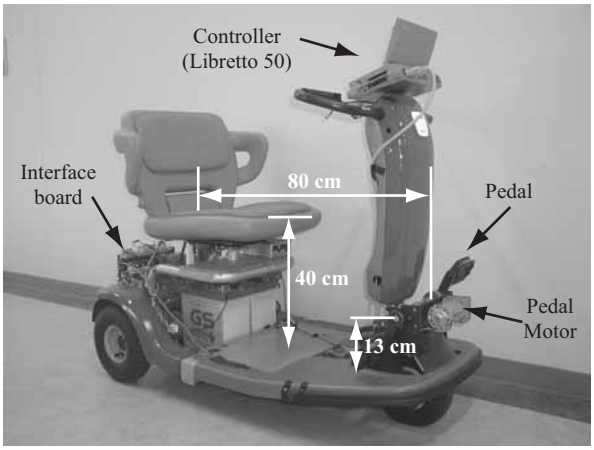

Fig. 7. Photograph of prototype electric cart.

A. Configuration of Control System

When the cart is driven, pushing the pedals generates a reference input for the cart; and the cart then moves and tracks the input signal. Hence, the cart system is a kind of cooperative man-machine system [13]–[15].

Regarding the structure of the cart control system, position, speed or force can be selected as the controlled output. Since a first-order plant is easy for people to operate in a cooperative man-machine system [16], speed was selected in our case. The system employs a master-slave configuration (e.g., [17]) to make the driving experience more realistic and to ease the driver's stress. When the driver pushes the pedals with torque $\tau(t)$, the pedal motor (master) turns with rotational speed $v_m(t)$. This is used as a reference speed for the cart motor (slave), which drives the cart. The speed at which the cart moves is proportional to the rotational speed, $v_s(t)$, of the cart motor. The error between $v_m(t)$ and $v_s(t)$ is fed back to the controller of the cart motor to generate a control input for it so that the speed of the cart motor can track the speed of the pedal motor.

In addition, to enable the driver to perform an appropriate level of physical exercise, the pedal motor can be set to make the pedals more difficult or easier to turn. And a bilateral scheme (e.g., [18], [19]) is used that also feeds the error between $v_m(t)$ and $v_s(t)$ back to the pedal motor, so that the driver can feel the road conditions and obtain a more realistic driving experience. The configuration of the bilateral master-slave cart system is shown in Fig. 8.

In this system, the speed at which the pedals turn the pedal motor is determined by the driver's efforts, and constitutes a reference input for the cart. The controller makes the speed of the cart motor track that reference. So, the experience is very similar to riding a bicycle.

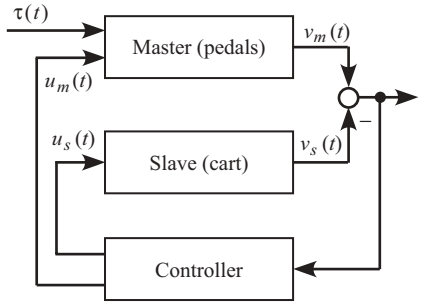

Fig. 8. Configuration of bilateral master-slave cart system.

B. Modeling

The pedal and cart systems have the same structure (Fig. 9).

The master (pedals) is described by the following equation:

$$\begin{cases} \dfrac{dv_m(t)}{dt} = A_m v_m(t) + B_m u_m(t) + B_\tau \tau(t), \\ A_m = -\dfrac{c_m}{J_m},\ B_m = \dfrac{k_m}{J_m},\ B_\tau = \dfrac{1}{J_m}. \end{cases} \tag{1}$$

Since it is difficult to determine B_τ in (1) precisely, a new variable, $\tau'(t) := B_\tau \tau(t)$, was introduced, which allows the mathematical model of the master to be rewritten as ($B'_\tau = 1$)

$$\frac{dv_m(t)}{dt} = A_m v_m(t) + B_m u_m(t) + B'_\tau \tau'(t). \tag{2}$$

The dynamics of the slave (cart) depend on the weight of the driver. The electric cart was originally designed for a driver weighing $45 \sim 100$ kg. This yields

$$\begin{cases} \dfrac{dv_s(t)}{dt} = A_s(t) v_s(t) + B_s(t) u_s(t), \\ A_s(t) = -\dfrac{c_s}{J_s(t)} := A_{s0} + \Phi \Gamma(t) \Psi_A, \\ B_s(t) = \dfrac{k_s}{J_s(t)} := B_{s0} + \Phi \Gamma(t) \Psi_B, \\ \Gamma^T(t)\Gamma(t) \le I. \end{cases} \tag{3}$$

In (1)–(3),

- $u_m(t)$ ($u_s(t)$): Voltage applied to the pedal (cart) motor [V].
- J_m ($J_s(t)$): Moment of inertia of the master (slave) motor [$\mathrm{kg \cdot m^2}$].
- c_m (c_s): Coefficient of viscous damping of the master (slave) [$\mathrm{kg \cdot m/s}$].
- k_m (k_s): Voltage transfer factor of the master (slave) motor driver [Nm/V].

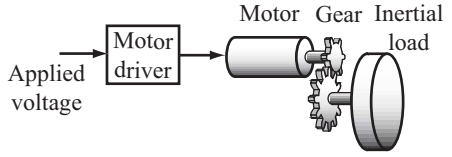

Fig. 9. Structure of master/slave.

The experimentally obtained values of the parameters are:

$$\begin{cases} A_m = -1.49, & B_m = 2.45, \\ A_{s0} = -0.24, & B_{s0} = 2.08, \\ \Phi = [1\ 1], & \\ \Psi_A = [0.04\ \ 0]^T, & \Psi_B = [0\ \ 0.69]^T. \end{cases} \tag{4}$$

C. Formulation of Control Problem

Instead of the load on the pedals being transmitted mechanically by means of a chain, the pedal and cart motors are connected electrically. The following impedance model describes the feeling of pushing the pedals:

$$\frac{dv_p(t)}{dt} = A_p v_p(t) + B_p \tau'(t), \tag{5}$$

where A_p and B_p are constants that determine the feeling. The system was set up with three sets of the parameters $[A_p,\ B_p]$ for three different modes of operation to suit the driver's physical condition:

$$\begin{cases} A_p = -1.49, & B_p = 2.00 \quad (\text{Mode A}: \text{ Strenuous Mode}); \\ A_p = -1.49, & B_p = 3.49 \quad (\text{Mode B}: \text{ Neutral Mode}); \\ A_p = -1.49, & B_p = 3.90 \quad (\text{Mode C}: \text{ Assisted Mode}). \end{cases} \tag{6}$$

We formulate the design problem for the controller using a common H_∞ control formulation. The exogenous input signal is $\tilde{\tau}(t) := [\tau'(t)\ \ \tau_\Gamma(t)]^T$, where $\tau_\Gamma(t)$ is the output signal of the uncertainty $\Gamma(t)$ (Fig. 10), and the controlled outputs are:

1) the weighted speed error between the impedance model and the pedals, $z_m(t)$;
2) the weighted speed error between the pedals and the wheels, $z_{ve}(t)$;
3) the input signal of the uncertainty $\Gamma(t)$, $z_\Gamma(t)$;
4) the weighted acceleration of the cart, $z_{as}(t)$, in order to take riding comfort into account; and
5) the weighted voltages applied to the pedal and cart motors, $z_{um}(t)$ and $z_{us}(t)$, in order to keep them at a low level.

The block diagram used for the design of the cart control system is shown in Fig. 10. Now, the design problem for the controller can be stated as follows:

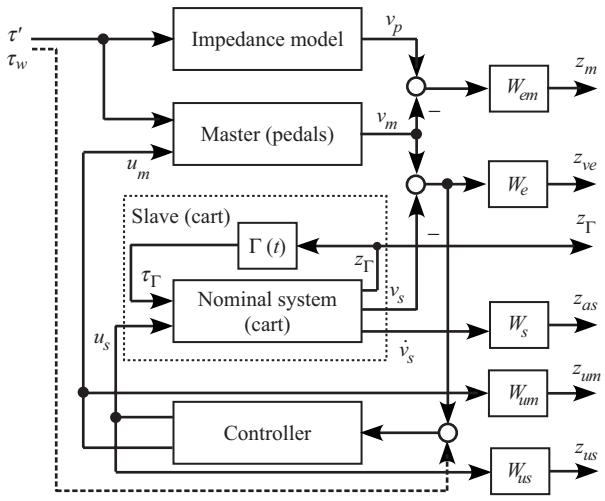

Fig. 10. Block diagram used for design of H_∞ controller.

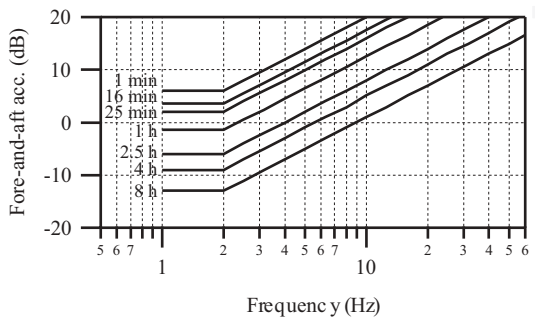

Fig. 11. Limits on whole-body vibrations in fore-and-aft direction to which operator is exposed [23], [24].

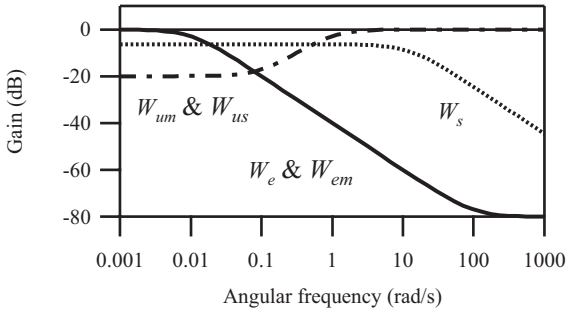

Fig. 12. Bode plots of weighting functions.

Find a controller $K(s)$ such that

1) *the cart control system is internally stable, and*
2) *the H_∞ norm of the transfer function from $\tilde{\tau}(t)$ to $z(t) := [z_m(t)\ z_{ve}(t)\ z_\Gamma(t)\ z_{as}(t)\ z_{um}(t)\ z_{us}(t)]^T$, $G_{z\tilde{\tau}}(s)$, is less than 1, i.e., $\|G_{z\tilde{\tau}}(s)\|_\infty < 1$.*

D. H_∞ Controller

To satisfy conditions (1) and (2) and to obtain an H_∞ controller that provides the desired performance, the following weighting transfer functions are used [20]–[22] in the design of the H_∞ controller:

$$\begin{cases} W_{em}(s) = W_e(s) = \dfrac{0.01s+1}{100s+1} = \left[\begin{array}{c|c} A_e & B_e \\ \hline C_e & D_e \end{array}\right], \\ W_{um}(s) = W_{us}(s) = \dfrac{s+0.1}{s+1} = \left[\begin{array}{c|c} A_u & B_u \\ \hline C_u & D_u \end{array}\right], \\ W_s(s) = \dfrac{0.48}{0.0812s+1} = \left[\begin{array}{c|c} A_a & B_a \\ \hline C_a & 0 \end{array}\right], \end{cases} \tag{7}$$

where $G(s) = D + C(sI - A)^{-1}B$ is abbreviated to $G(s) = \left[\begin{array}{c|c} A & B \\ \hline C & D \end{array}\right]$. In order to suppress the tracking error between $v_p(t)$ and $v_m(t)$ and that between $v_m(t)$ and $v_s(t)$ in the steady state, low-pass weighting functions were chosen for $W_{em}(s)$ and $W_e(s)$. To suppress the applied control voltages, $u_m(t)$ and $u_s(t)$, to the pedal and cart motors during the transient response, high-pass weighting functions were chosen for $W_{um}(s)$ and $W_{us}(s)$.

Ride comfort is also a very important criterion in evaluating control. The limits on the vibrations to which an operator should be exposed are given in [23], [24]. Since the cart is designed to be used mainly on paved sidewalks, the effect of whole-body vibration in the fore-and-aft direction on ride comfort is taken into account. Fig. 11 shows the limits for this type of vibration [23], [24]. A direct calculation shows that the curves in Fig. 11 can be approximated by the transfer function $W_{s(\mathrm{ISO})}(s) = (0.0812s+1)/\alpha$, where α is a constant decided by the duration of exposure. Hence, the weighting function for evaluating ride comfort has the form $W_s(s) = \bar{\alpha}/(0.0812s+1)$, where $\bar{\alpha}$ is a gain factor used to adjust the weighting function. $\bar{\alpha}$ was tuned through trial and error, and was finally set to 0.48. Bode plots of the weighting transfer functions are shown in Fig. 12.

In order to relax the solvable condition and obtain a satisfactory H_∞ controller, a disturbance, $\tau_w(t)$, was added to the measurement output channel. Finally, the generalized plant is given by

$$\left[\begin{array}{c} \dot{x}(t) \\ \hline z(t) \\ y(t) \end{array}\right] = \left[\begin{array}{c|cc} A & B_1 & B_2 \\ \hline C_1 & 0 & D_{12} \\ C_2 & D_{21} & 0 \end{array}\right] \left[\begin{array}{c} x(t) \\ \hline w(t) \\ u(t) \end{array}\right], \tag{8}$$

where

$$\begin{aligned} x(t) &:= [v_p(t)\ v_m(t)\ v_s(t)\ x_m(t)\ x_{ve}(t)\ x_{as}(t) \\ &\qquad x_{um}(t)\ x_{us}(t)]^T, \\ w(t) &:= [\tau'(t)\ \tau_\Gamma(t)\ \tau_w(t)]^T, \\ u(t) &:= [u_m(t)\ u_s(t)]^T, \\ y(t) &:= v_m(t) - v_s(t) + \tau_w(t), \end{aligned}$$

$x_m(t)$, $x_{ve}(t)$, $x_{as}(t)$, $x_{um}(t)$ and $x_{us}(t)$ are the states of the weighting functions $W_{em}(s)$, $W_e(s)$, $W_s(s)$, $W_{um}(s)$ and $W_{us}(s)$, respectively, and

$$A = \begin{bmatrix} A_p & 0 & 0 & 0 & 0 & 0 & 0 & 0 \\ 0 & A_m & 0 & 0 & 0 & 0 & 0 & 0 \\ 0 & 0 & A_{s0} & 0 & 0 & 0 & 0 & 0 \\ B_e & -B_e & 0 & A_e & 0 & 0 & 0 & 0 \\ 0 & B_e & -B_e & 0 & A_e & 0 & 0 & 0 \\ 0 & 0 & B_a A_{s0} & 0 & 0 & A_a & 0 & 0 \\ 0 & 0 & 0 & 0 & 0 & 0 & A_u & 0 \\ 0 & 0 & 0 & 0 & 0 & 0 & 0 & A_u \end{bmatrix},$$

$$B_1^T = \begin{bmatrix} B_p^T & {B'_\tau}^T & 0 & 0 & 0 & 0 & 0 & 0 \\ 0 & 0 & \Phi^T & 0 & 0 & (B_a\Phi)^T & 0 & 0 \\ 0 & 0 & 0 & 0 & 0 & 0 & 0 & 0 \end{bmatrix},$$

$$B_2^T = \begin{bmatrix} 0 & B_m^T & 0 & 0 & 0 & 0 & B_u^T & 0 \\ 0 & 0 & B_{s0}^T & 0 & 0 & (B_a B_{s0})^T & 0 & B_u^T \end{bmatrix},$$

$$C_1 = \begin{bmatrix} D_e & -D_e & 0 & C_e & 0 & 0 & 0 & 0 \\ 0 & D_e & -D_e & 0 & C_e & 0 & 0 & 0 \\ 0 & 0 & \Psi_A & 0 & 0 & 0 & 0 & 0 \\ 0 & 0 & 0 & 0 & 0 & C_a & 0 & 0 \\ 0 & 0 & 0 & 0 & 0 & 0 & C_u & 0 \\ 0 & 0 & 0 & 0 & 0 & 0 & 0 & C_u \end{bmatrix},$$

$$C_2 = \begin{bmatrix} 0 & 1 & -1 & 0 & 0 & 0 & 0 & 0 \end{bmatrix},$$

$$D_{12}^T = \begin{bmatrix} 0 & 0 & 0 & 0 & D_u^T & 0 \\ 0 & 0 & \Phi_B^T & 0 & 0 & D_u^T \end{bmatrix},$$

$$D_{21} = \begin{bmatrix} 0 & 0 & 1 \end{bmatrix}.$$

Clearly,

- (A, B_2) is stabilizable and (C_2, A) is detectable;

- D_{12} has full column rank and D_{21} has full row rank;
- $\left[\begin{array}{c|c} A-j\omega I & B_2 \\ \hline C_1 & D_{12} \end{array}\right]$ has full column rank for all ω; and
- $\left[\begin{array}{c|c} A-j\omega I & B_1 \\ \hline C_2 & D_{21} \end{array}\right]$ has full raw rank for all ω.

So, it is a standard H_∞ control problem, and an H_∞ controller is easily obtained using existing H_∞ solvers [25], [26]. In this study, we used the LMI approach to design a controller. It is known that an H_∞ controller guaranteeing that $\|G_{zw}(s)\|_\infty < 1$ ($G_{zw}(s)$ is the transfer function from $w(t)$ to $z(t)$) exists if and only if $\mathcal{L}_D \neq \emptyset$ [27]–[29], where

$$\mathcal{L}_D := \Big\{ (X,Y) \in \Re^{8\times 8} \times \Re^{8\times 8} : X > 0,\ Y > 0,$$
$$L_B(X) < 0,\ L_C(Y) < 0,\ \begin{bmatrix} X & I \\ I & Y \end{bmatrix} \geq 0 \Big\},$$
$$L_B(X) = \begin{bmatrix} B_2 \\ D_{12} \end{bmatrix}^{\perp} Q_X \begin{bmatrix} B_2 \\ D_{12} \end{bmatrix}^{\perp T},$$
$$L_C(Y) = \begin{bmatrix} C_2^T \\ D_{21}^T \end{bmatrix}^{\perp} Q_Y \begin{bmatrix} C_2^T \\ D_{21}^T \end{bmatrix}^{\perp T},$$
$$Q_X = \begin{bmatrix} AX + XA^T + B_1B_1^T & XC_1^T + B_1D_{11}^T \\ C_1X + D_{11}B_1^T & D_{11}D_{11}^T - I \end{bmatrix},$$
$$Q_Y = \begin{bmatrix} YA + A^TY + C_1^TC_1 & YB_1 + C_1^TD_{11} \\ B_1^TY + D_{11}^TC_1 & D_{11}^TD_{11} - I \end{bmatrix}.$$

The H_∞ synthesis problem was solved with the solver `hinflmi` in the LMI Toolbox [26].

Remark 1: The disturbance $\tau_w(t)$ is not needed when the LMI approach is used to solve the H_∞ control problem. However, a comparison of the results for the designed control system with and without $\tau_w(t)$ revealed that, in our system, the controller obtained with $\tau_w(t)$ suppressed uncomfortable vibrations in the frequency band to which human beings are sensitive more than the one without $\tau_w(t)$. Thus, we kept $\tau_w(t)$ in our design.

V. Experiments

The effectiveness of pedaling as a way of maintaining or improving physical strength, the usability of the system architecture, and the validity of the designed H_∞ controller were verified through experiments. A Libretto 50 notebook computer (CPU: 75-MHz Pentium; Memory: 16 MB; Toshiba) was used for the controller. Since the control information is handled by the interface board, the implementation of the controllers is very simple. Even a low-performance computer, such as that used in the experimental system, is sufficient to control the system. This demonstrates the rationality of the system configuration. In fact, since the interface board can be programmed to perform various functions for system integration and since many resources on the board remain available for further development, the board can be used not only to handle the inputs and outputs intelligently but also to monitor and supervise the driver's physical condition.

Each of the three impedance modes (A, B, C) (6) was tested under three road conditions: flat road, 5° uphill slope, and 5° downhill slope for a driver weight range of $47 \sim 70$ kg.

Typical experimental results are shown in Figs. 13–15 for a driver weighing 63 kg. Figure 13 is for a flat road. In this case,

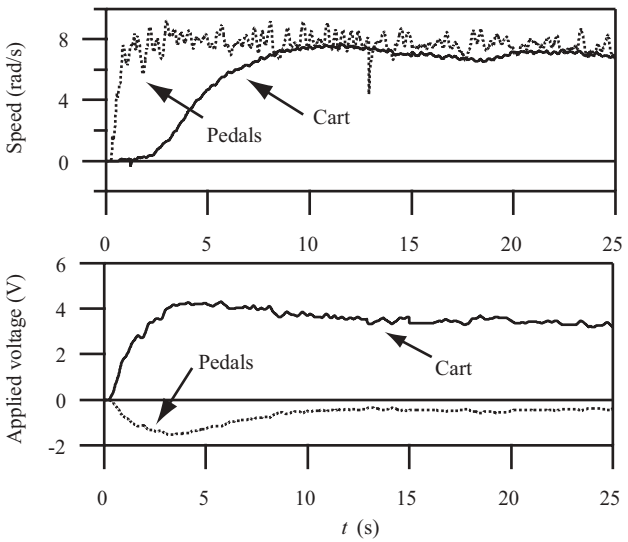

(a) Mode A (Strenuous Mode).

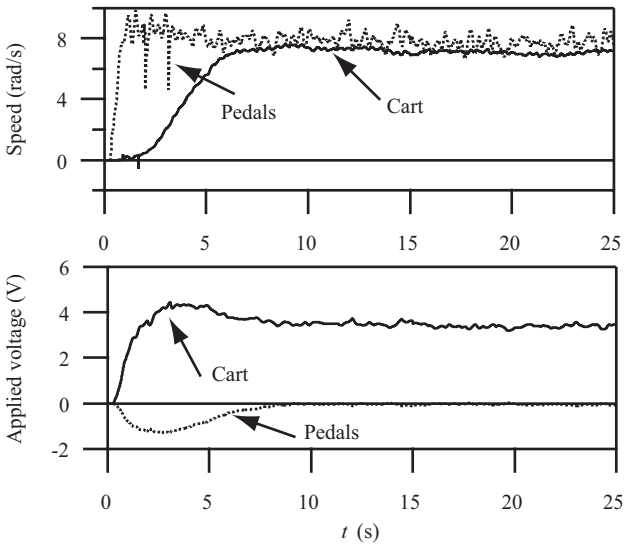

(b) Mode B (Neutral Mode).

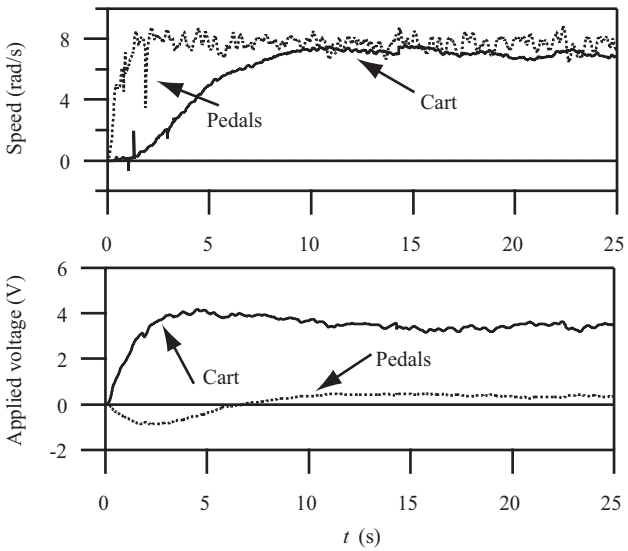

(c) Mode C (Assisted Mode).

Fig. 13. Experimental results for flat road.

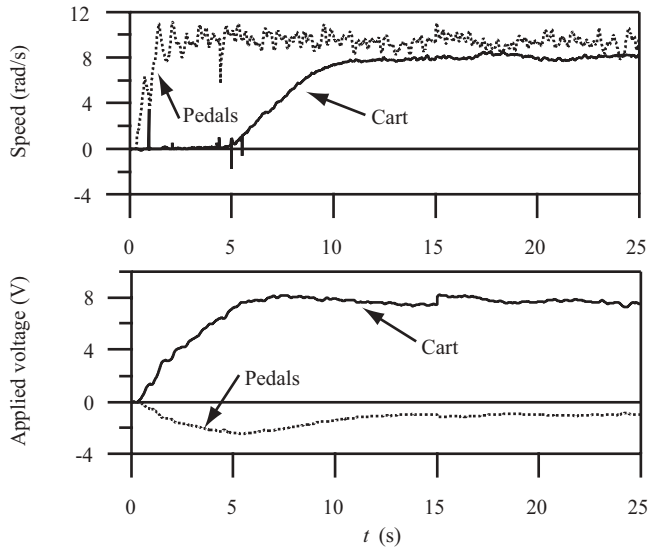

(a) Mode A (Strenuous Mode).

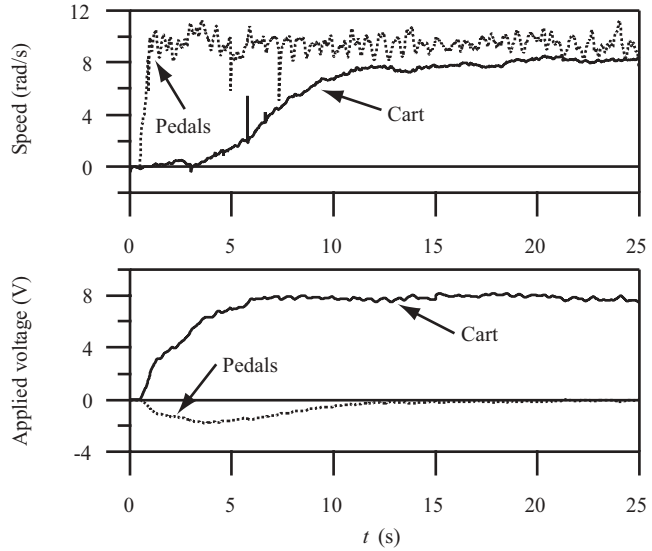

(b) Mode B (Neutral Mode).

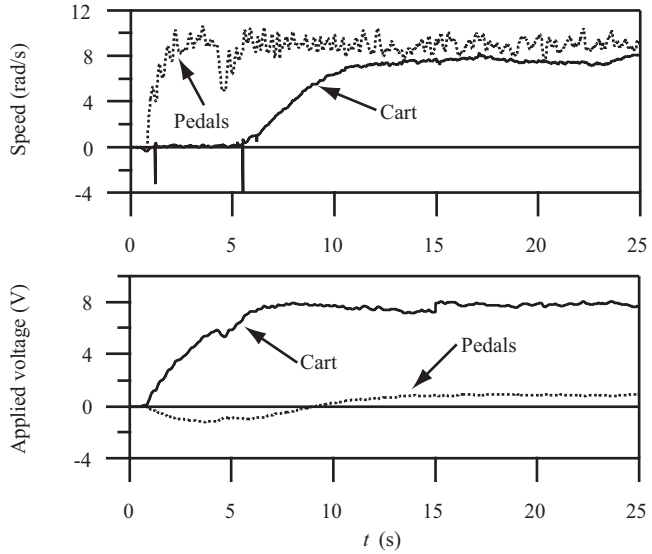

(c) Mode C (Assisted Mode).

Fig. 14. Experimental results for uphill slope.

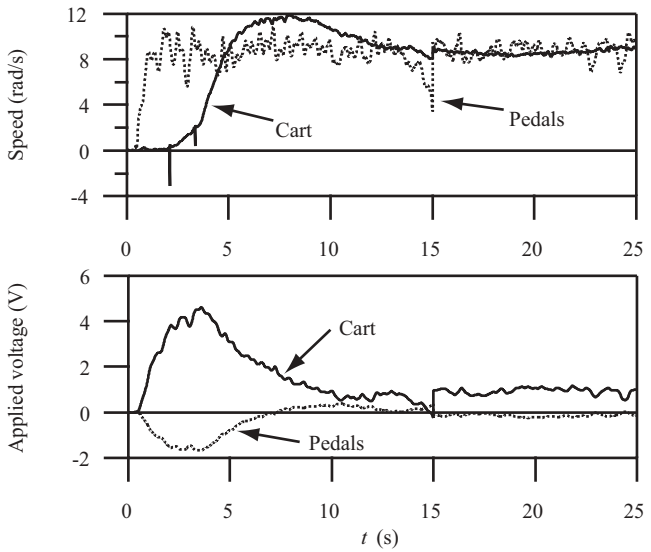

(a) Mode A (Strenuous Mode).

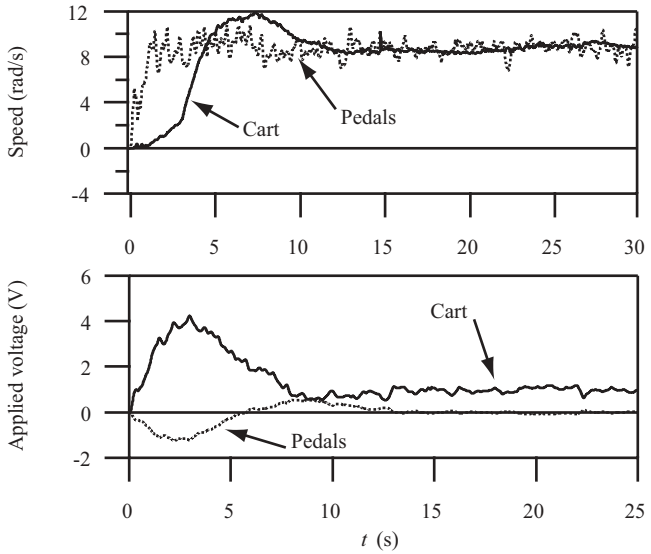

(b) Mode B (Neutral Mode).

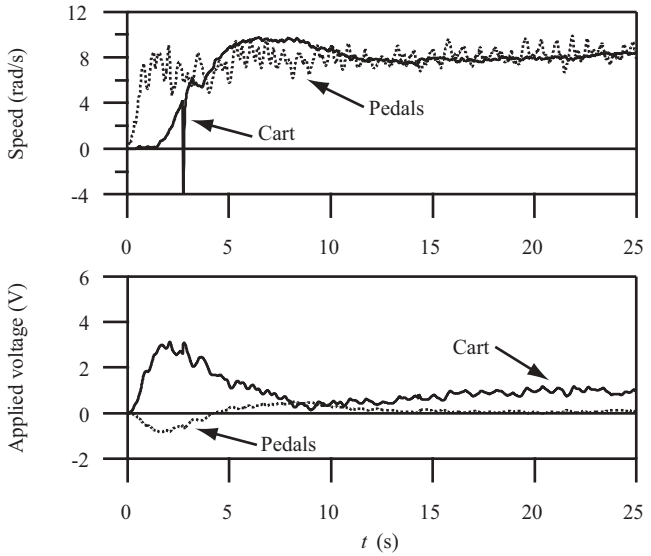

(c) Mode C (Assisted Mode).

Fig. 15. Experimental results for downhill slope.

TABLE II
AVERAGE INPUT VOLTAGES DURING THE PERIOD 15-25 S.

	Strenuous Mode	Neutral Mode	Assisted Mode
Flat	-0.462	-0.047	0.377
Uphill	-0.993	-0.088	0.866
Downhill	-0.105	0.003	0.097

during the steady state (the period $[15\ \mathrm{s},\ 25\ \mathrm{s}]$), the average input voltages to the cart produced by the H_∞ controller were -0.462 V, -0.047 V, and 0.377 V for Modes A, B, and C, respectively. The negative value for Mode A means that an extra load was produced for the driver, making the pedals more difficult to turn. Note that a relatively large load was produced in the transient response for a few seconds. It is helpful to provide the driver with anaerobic exercise to ensure that both fast- and slow-twitch fibers are exercised in a balanced way. On the other hand, Mode B produced virtually no load because the average input voltage was almost zero. And the positive value for Mode C means that the driver was assisted. The 2-Hz oscillation in the speed of the pedals is due to the driver's pushing the pedals.

The results for the uphill slope are shown in Fig. 14. The average voltages during the steady state (the period $[15\ \mathrm{s},\ 25\ \mathrm{s}]$) were -0.993 V, -0.088 V, and 0.866 V for Modes A, B, and C, respectively. While the Neutral Mode (Mode B) guaranteed that the voltage input to the pedal motor remained at a very low level, Modes A and C provided a larger extra load or more assistance to the driver than those for the flat road. This reflected the actual road conditions and gave the driver more of a feeling of really driving, thus providing more sensory stimulation.

The results for the downhill slope are shown in Fig. 15. The average voltages during the steady state (the period $[15\ \mathrm{s},\ 25\ \mathrm{s}]$) were -0.105 V, 0.003 V, and 0.097 V for Modes A, B, and C, respectively. Note that, in this case, while the voltage input to the cart in the Neutral Mode (Mode B) still remained at a very low level, Modes A and C provided a smaller extra load or less assistance to the driver than those for the flat road. Thus, the system is responsive to the road conditions.

The average input voltages for the various conditions and modes during the steady state (15-25 s) are listed in Table II.

VI. CONCLUSIONS

A new type of three-wheeled electric cart has been developed to maintain or improve the physical strength of the elderly. It features an ergonomically designed pedal unit that provides exercise for the muscles of the lower limbs, which tend to degenerate most rapidly due to aging. An electrical rather than a mechanical connection is employed between the pedals and the drive wheels to enhance flexibility. An interface board was assembled to intelligently handle the inputs and outputs of the system and to lighten the burden on the control computer. The board includes a PIC microcontroller that allows the system to be augmented with a great variety of functions. An impedance model is used to describe the feeling of pushing the pedals; and a bilateral master-slave control system based on that model was built to control the speed of the cart. So, unlike most of the electric carts that are currently available, this one not only is a vehicle, but also provides the driver with physical exercise. The controller was designed using H_∞ control theory. The effectiveness of the cart and the system architecture, and the validity of the designed H_∞ controller were tested under various load and road conditions. Experimental results show that this system configuration is very rational and that the cart is useful for providing an appropriate level of physical exercise. A final point is that this electric cart is also beneficial for people undergoing rehabilitation.

ACKNOWLEDGMENTS

The authors would like to thank Tetsuya Suzuki of Sigmatron Co. Ltd., Kiyoto Doi of Japan Business Development Inc., Takaaki Tobari of Toshin Electric Co., Ltd., Keigo Tsuji of Nihon Medix Co., Ltd., and Hiroki Yamamoto of Kikuchi Works Co. Ltd. for their contribution to this study.

REFERENCES

[1] Cabinet Office, *Annual Report on the Aging Society: 2004 (Summary)*, 2004. [online]. Available: http://www8.cao.go.jp/kourei/

[2] H. Mori, S. Kotani and N. Kiyohiro, "HITOMI: Design and Development of a Robotic Travel Aid," in *Assistive Technology and Artificial Intelligence –Applications in robotics, user interfaces and natural language processing–*, V. O. Mittal, H. A. Yanco, J. Aronis, and R. Simpson Eds. Springer-Verlag, Berlin, 1998, pp. 221–234.

[3] R. A. Cooper and R. Cooper, "Trends and Issues in Wheeled Mobility Technologies," *Space Requirements for Wheeled Mobility Workshop*, Center for Inclusive Design and Environmental Access, 2003. [online]. Available: http://www.ap.buffalo.edu/idea/space%20workshop/papers.htm

[4] T. Fukunaga, "Age and sex differences in Japanese life fitness," *Japanese J. Physical Fitness & Sports Medicine*, vol. 52, Suppl. pp. 9-16, 2003. (in Japanese)

[5] S. Kuno, H. Murakami, S. Baba, J. Kim and M. Kamioka, "Effect of strength training on aging muscles of elderly people," *Japanese J. Physical Fitness & Sports Medicine*, vol. 52, Suppl. pp. 17-30, 2003. (in Japanese)

[6] M. P. Murray, "Gait as a total pattern of movement," *American J. Phys. Med.*, vol. 46, pp. 290-333, 1967.

[7] National Institute on Aging: *Exercise: a guide from the National Institute on Aging*, 2001. [online]. Available: http://www.niapublications.org/exercisebook/ExerciseGuideComplete.pdf

[8] D. A. Brown, S. A. Kautz and C. A. Dairaghi, "Muscle activity patterns altered during pedaling at different body orientations," *J. Biomechanics*, vol. 29, pp. 1349-1356, 1996.

[9] Research Institute of Human Engineering for Quality Life, *Database of fundamental improvement for the elderly*, 2003. [online]. Available (in Japanese): http://www.hql.jp/gpd/jpn/www/13web2000/ 2000top.htm

[10] C. T. Morgan, J. S. Cook III, A. Chapanis and M. W. Lund, *Human engineering guide to equipment design*, New York: McGraw-Hill Book, 1963.

[11] Microchip, *PIC15C7X: 8-Bit CMOS Microcontrollers with A/D Converter*, 2002, [online]. Available: http://ww1.microchip.com/downloads/en/DeviceDoc/30390e.pdf

[12] Toshiba, *TA7272*, 1997, [online]. Available: http://www.alldatasheet.net/datasheet-pdf/pdf/TOSHIBA/TA7272.html

[13] G. Schweitzer, "Mechatronics for the design of human-oriented machines," *IEEE/AMSE Trans. Mechatron.*, vol. 1, pp. 120–126, Jun. 1996.

[14] T. Inaba, M. Hayashizaki and Y. Matsuo, "Design of a Human-Machine Cooperation System to Facilitate Skilled Work," *Proc. 1997 IEEE Int. Conf. Syst., Man, Cybern.*, vol. 4, pp. 995–1000, 1999.

[15] P. M. Jones and J. L. Jacobs, "Cooperative Problem Solving in Human-Machine Systems: Theory, Models, and Intelligent Associate Systems," *IEEE Trans. Syst., Man, Cybern. C*, vol. 30, pp. 397–407, Nov. 2000.

[16] T. Inaba and Y. Matsuo, "Loop-shaping Characteristics of a Human Operator in a Force Reflective Manual Control System," *Proc. 1997 IEEE Int. Conf. Syst., Man, Cybern.*, pp. 3621-3625, 1997.
[17] H. Kazerooni, T.-I. Tsay and K. Hollerbach, "A Controller Design Framework for Telerobotic Systems," *IEEE Trans. Contr. Syst. Technol.*, vol. 1, pp. 50-62, Mar. 1993.
[18] Y. Yokokohji and T. Yoshikawa, "Bilateral Control of Master-Slave Manipulators for Ideal Kinesthetic Coupling—Formulation and Experiment," *IEEE Trans. Robot. Automat.*, vol. 5, pp. 605-620, Oct. 1994.
[19] W.-H. Zhu and S. E. Salcudean, "Stability Guaranteed Teleoperation: An Adaptive Motion/Force Control Approach," *IEEE Trans. Automat. Contr.*, vol. 45, pp. 1951-1969, Nov. 2000.
[20] M. G. Ortega and F. R. Rubio, "Systematic design of weighting matrices for the H_∞ mixed sensitivity problem," *J. Process Control*, vol. 14, pp. 89-98, 2004.
[21] T. Hiromatsu, T. Inaba and Y. Matsuo, "Development of an Electromechanical Active-Cab-Suspension," *Proc. IEEE Int. Conf. on Industrial Electronics, Control, and Instrumentation (IECON'93)*, pp. 2132-2137, 1993.
[22] J. Yan and S. E. Salcudean, "Teleoperation Controller Design Using H_∞ Optimization with Application to Motion-Scaling," *IEEE Trans. Contr. Syst. Technol.*, vol. 4, pp. 244-258, May 1996.
[23] M. J. Griffin, *Handbook of Human Vibration*, San Diego, California: Elsevier Ltd., 1990.
[24] G. Salvendy, *Handbook of Human Factors and Ergonomics*, 2nd Ed., New York: John Wiley & Sons, Inc., 1997.
[25] R. Y. Chiang and M. G. Safonov, *Robust Control Toolbox*, Natick, MA: The MathWorks, 1996.
[26] P. Gahinet, A. Nemirovski, A. J. Laub and M. Chilali, *LMI Control Toolbox*, Natick, MA: The MathWorks, 1995.
[27] T. Iwasaki and R. E. Skelton, "All controllers for the general H_∞ control problem: LMI existence conditions and state space formulas," *Automatica*, vol. 30, pp. 1307-1317, 1994.
[28] K. Zhou, J. C. Doyle and K. Glover, *Robust and Optimal Control*, Upper Saddle River, New Jersey: Prentice-Hall, Inc., 1996.
[29] X. Xin, "Reduced-order controllers for the H_∞ control problem with unstable invariant zeros," *Automatica*, vol. 40, pp. 319-326, 2004.

PLACE PHOTO HERE

Jin-Hua She (M'94) received a B.S. in engineering from Central South University, Changsha, China, in 1983, and an M.S. in 1990 and a Ph.D. in 1993 in engineering from the Tokyo Institute of Technology, Tokyo, Japan. In 1993, he joined the Department of Mechatronics, School of Engineering, Tokyo University of Technology; and in April, 2004 he transferred to the University's School of Bionics, where he is currently an associate professor. He received the control engineering practice paper prize of IFAC in 1999 (jointly with M. Wu and M. Nakano). His current research interests include the application of control theory, repetitive control, expert control, Internet-based engineering education, and robotics. He is a member of the Society of Instrument and Control Engineers (SICE) and the Institute of Electrical Engineers of Japan (IEEJ).

PLACE PHOTO HERE

Yasuhiro Ohyama received BS, MS and PhD degrees in Engineering from the Tokyo Institute of Technology, Tokyo, Japan in 1980, 1982 and 1985, respectively. He worked on developing controllers for industrial robots and on CAD systems for control design as a director of Advanced Control Laboratory Inc., Tokyo, Japan from 1985 to 1991. He is currently a professor at the School of Bionics, Tokyo University of Technology, where he does research on the application of control theory, robotics, and engineering education. He is a member of the Society of Instrument and Control Engineers (SICE) and the Institute of Electrical Engineers of Japan (IEEJ).

PLACE PHOTO HERE

Hiroyuki Kobayashi received MS and Ph.D. degrees in Engineering from Tokyo Institute of Technology, Japan in 1996 and 2003, respectively. In 2001, he joined the Department of Environmental Information, Keio University. In 2003, he transferred to the School of Bionics, Tokyo University of Technology, where he is currently a research assistant. His research interests include multi-agent robotics and man-machine systems. He is a member of the Robotics Society of Japan (RSJ), the Society of Instrument and Control Engineers (SICE), and the Institute of Electrical Engineers of Japan (IEEJ).